

Zero Experience Required: Plug & Play Modular Transfer Learning for Semantic Visual Navigation

Ziad Al-Halah¹ Santhosh K. Ramakrishnan^{1,2} Kristen Grauman^{1,2}

¹The University of Texas at Austin ²Facebook AI Research

ziadlhlh@gmail.com, srama@cs.utexas.edu, grauman@cs.utexas.edu

Abstract

In reinforcement learning for visual navigation, it is common to develop a model for each new task, and train that model from scratch with task-specific interactions in 3D environments. However, this process is expensive; massive amounts of interactions are needed for the model to generalize well. Moreover, this process is repeated whenever there is a change in the task type or the goal modality. We present a unified approach to visual navigation using a novel modular transfer learning model. Our model can effectively leverage its experience from one source task and apply it to multiple target tasks (e.g., ObjectNav, RoomNav, ViewNav) with various goal modalities (e.g., image, sketch, audio, label). Furthermore, our model enables zero-shot experience learning, whereby it can solve the target tasks without receiving any task-specific interactive training. Our experiments on multiple photorealistic datasets and challenging tasks show that our approach learns faster, generalizes better, and outperforms SoTA models by a significant margin.

1. Introduction

In visual navigation, an agent must intelligently move around in an unfamiliar environment to reach a goal, using its egocentric camera to avoid obstacles and decide where to go next. As a fundamental research problem in embodied AI, visual navigation has many potential applications—such as service robots in the home or workplace, mobile search and rescue robots, assistive technology for the visually impaired, and augmented reality systems to help people navigate or find objects.

Recent work in computer vision explores visual navigation from many different fronts. In PointNav, an agent is asked to go to a specific position in an unmapped environment (e.g., go to (x, y)) [6, 56, 57]. In ObjectNav, the agent must find an object by name (e.g., go to the nearest telephone) [6, 10]. In RoomNav, the agent must find

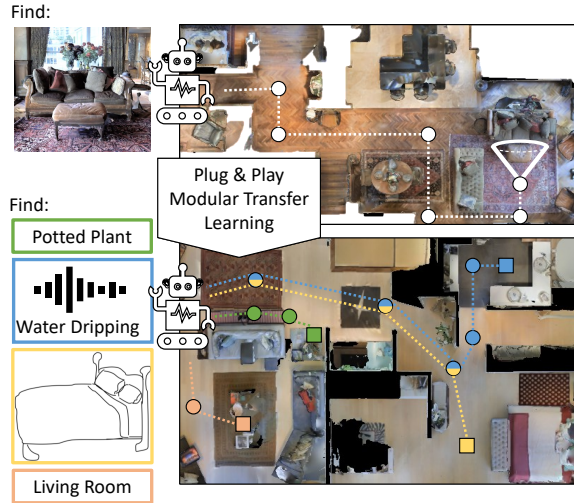


Figure 1. Our novel modular transfer learning approach for semantic visual navigation learns a general purpose semantic search policy by finding image views sampled randomly in the environment (top). Then, this experience is leveraged to search for previously unseen types of goals and search tasks (bottom). Our approach enables zero-shot experience learning (*i.e.*, perform the target task without receiving any new experiences) and it adapts its policy much faster using fewer target-specific interactions.

a room (e.g., go to the kitchen) [50, 56, 65]. In AudioNav, the agent must find a sounding target (e.g., find the ringing phone) [17, 29]. In ImageNav, the agent must go to where a given photo was taken [15, 55, 72]. Each case presents a distinct goal to the agent. Accordingly, researchers have pursued *task-specific* models to treat each one, typically training policies with deep reinforcement learning (RL).

Despite exciting advances, learning task-specific navigation policies has inherent limitations. Training embodied agents from scratch for each new task and relying on special-purpose architectures and priors (e.g., room layout maps for RoomNav, object co-occurrence priors for ObjectNav, directional cues for AudioNav, etc.) requires repeated access to training environments for gathering new agent experience in the context of each task, greatly hindering sam-

ple efficiency. Even with today’s fast simulators and photorealistic scanned environments [13, 57, 66], this typically amounts to days and weeks of computation on a small army of GPU servers to train a single policy. Moreover, by tackling each variant in isolation, agents fail to capture what is common across the tasks. Finally, some tasks require manual annotations such as object labels in 3D space, which naturally limits how extensively they can be trained.

In this work, we challenge the assumption that distinct navigation tasks require distinct policies. Intuitively, finding a good policy for one navigation task should help with the rest. For example, if we know how to find a microwave, then finding a kitchen should be easy too; if we know how to find an object by name, then finding it based on a hand-drawn sketch—or the sounds it emits—should be possible too. In short, it should be beneficial to learn one navigation task and then apply the accumulated experience to many.

To that end, we propose a modular transfer learning approach for semantic visual navigation that enables *zero-shot experience learning*. See Figure 1. First, we develop a general-purpose semantic search policy. Specifically, using a novel reward and task augmentation strategy, we train a source policy for the *image-goal* task, where the agent receives a picture taken at some unknown camera pose somewhere in the environment, and must travel to find it. Next, we develop a joint goal embedding that is trained offline (*i.e.*, no interactive agent experience) to relate various target goal types to image-goals. Finally, we address target downstream tasks either by zero-shot transfer with no new agent experience, or by fine-tuning with a limited amount of agent experience on the target task.

Zero-shot learning traditionally focuses on supervised tasks such as image recognition [5, 40, 67], where models forgo using labeled samples for the new class. Instead, the proposed zero-shot *experience learning* (ZSEL) focuses on reinforcement learning tasks, where models forgo using interactions in the physical environment for the new navigation task. We believe that ZSEL is important for lifelong learning, where an agent will face novel tasks once it is deployed and must solve them while using no or few training episodes.

Using hundreds of multi-room environments from Matterport3D [13], Gibson [66], and HM3D [52], we demonstrate our approach for four challenging tasks and goals expressed with five different modalities—images, category names, audio, hand-drawn sketches, and edgemaps. Our ImageNav results advance the state of the art, and our modular transfer approach outperforms existing forms of transfer based on self-supervision, supervision, and RL. Finally, our ZSEL performance on 5 semantic navigation tasks is equivalent to 507 million interactions required by task-specific policies learned from scratch.

2. Related Work

Visual Navigation Traditional methods in visual navigation often rely on mapping the 3D space and then planning their movements [9, 28, 61]. However, fueled by fast simulators [37, 57] and large-scale photorealistic datasets [13, 17, 52, 66] there have been great advances in learning-based navigation approaches [15, 18, 51] leading to a near-perfect agent for tasks like point-goal navigation [63]. In this work, we consider semantic visual navigation, where the agent is given a semantic description of the goal (*e.g.*, object-goal [6, 10], image-goal [15, 72], room-goal [65], audio-goal [16, 17]) but, unlike point-goal, the goal location is unknown. Hence, the agent needs to leverage learned scene priors to explore the environment efficiently to find and navigate to the target. Current approaches tackle each navigation task separately: a new model is trained for each task and each target modality [10, 15, 16, 65], which has the disadvantages discussed above. In contrast, we propose a unified approach to semantic visual navigation, in which a *single* trained policy can handle diverse tasks and goal modalities.

Transfer Learning in Navigation Pre-learning a representation from large-scale image datasets [22, 44] and transferring it to a downstream task proved to be very successful for visual recognition [11, 19, 20, 30, 70]. We observe a similar trend in embodied navigation where pre-learning good representations of the 3D environment [48, 49, 53, 68, 71] or primitive skills [26, 31, 43, 63] help the agent to learn a downstream task better while using fewer training samples. Recent methods focus on pre-training the observation encoder of the agent, either in a supervised [31, 58] or self-supervised [20, 23] fashion. While this leads to improved performance on the target tasks, a new policy is still learned from scratch for each task, resulting in low sample efficiency. In contrast, our approach enables a full transfer paradigm where all of the agent’s components can be reused efficiently on the downstream tasks. Prior work shows that transferring a strong point-goal policy to non-goal driven tasks (*e.g.*, flee and exploration) can lead to better performance [63]. Differently, we propose to learn and transfer a general-purpose semantic search policy. Our policy can find semantic goals presented in different modalities for a diverse set of goal-driven navigation tasks.

Sharing knowledge between multiple tasks can be achieved in a multi-task learning setup [14, 62] where all tasks are learned jointly in a supervised manner, or via meta-RL [27, 64] where a meta policy learned from a distribution of tasks is finetuned on the target. Unlike these methods, our policy is learned from one task that does not require manual annotations, and it can be transferred in a zero-shot setup where the policy does not receive any interactive training on the target.

Zero-Shot Learning Zero-shot learning (ZSL) can be seen as an extreme case of transfer learning where the target task has zero training samples. Prior ZSL work focuses on supervised learning, e.g., image classification [4, 5, 25, 40, 41, 54, 67]. In contrast, the proposed *zero-shot experience learning* (ZSEL) setup learns *behaviors* rather than classifiers; the policy learned on a source task needs to perform a set of target tasks, without receiving any new interactive experiences on the target. Further, unlike [60] where a world model for synthetic environments is constructed and control policies are trained on ‘imagined’ episodes, we consider a model-free approach and a ZSEL setup in realistic environments where the policy receives zero target interactions (*i.e.*, neither imagined nor real). To our knowledge, we are first to propose a ZSEL model for embodied navigation.

3. Plug & Play Modular Transfer Learning

We introduce a novel transfer learning approach for visual navigation. Our model has three main components: 1) we start by learning a semantic search policy for image goals using a novel reward and task augmentation (Fig. 2a); 2) we leverage the image goal encoder to learn a joint goal embedding space for the different goal modalities (Fig. 2b); and finally, 3) we transfer the learned agent modules to downstream tasks in a plug and play fashion (Fig. 2c).

In the following, we consider an agent with 3 main modules: 1) an observation encoder (f_O) that encodes the received observations o_t from the environment; 2) a goal encoder (f_G) that encodes the task’s goal; 3) a policy (π) that uses the output of f_O and f_G to navigate and find the goal.

3.1. Semantic Search Policy for Image Goals

The policy is a key component in the modern end-to-end visual navigation agent. It guides the agent towards solving a task given a set of sequential observations and a goal. Such policies are often learned with reinforcement learning (RL) where the agent interacts with its environment (by moving about) and attempts to solve the task in a trial and error fashion. If the agent succeeds in its attempt, then it receives a reward to encourage such behavior from the policy in the future.

A main challenge for this learning paradigm is that the policy requires a large number of interactions with the environment in order to find a proper way to solve the task. This usually amounts to tens and hundreds of millions [45, 46] and up to billions [63] of interactions, and correspondingly days or weeks of GPU cluster time. Furthermore, for each new task a policy is typically learned from scratch, which further increases the learning cost substantially.

We propose to learn a general-purpose *semantic search* policy that can be transferred and perform well on a variety of navigation tasks. Our idea is to learn such a policy

with the image-goal task, where the agent receives a picture taken at some unknown camera pose somewhere in the environment, and must travel to find it. Our choice of image-goal for the source policy is significant. It requires no manual annotations, and image-goals can be sampled freely anywhere in a training environment. As a result, the policy can be trained on large-scale experience (*e.g.*, collected from a fleet of robots deployed in various environments) which can improve its generalization to new tasks and domains. Furthermore, an image-goal encourages the learned policy to capture semantic priors for finding things in a 3D space. For example, by seeking images of couches and chairs, the agent learns implicitly to leverage these objects’ context and the room layout in order to find the image views effectively.

Task Definition In an episode of image goal navigation, the agent starts from a random position p_0 in unexplored scene and it is tasked to find a certain location p_G given an image I_G sampled with the camera at p_G . The agent receives an RGB observation o_t at each step t and needs to perform the best sequence of actions $a_t \in \{\text{move_forward, turn_left, turn_right, stop}\}$ that would bring it to the goal within a maximum number of steps S . Unlike the common point-goal task where the goal location is known [6], here p_G is unknown and the agent needs to leverage the learned semantic priors to search and find where I_G could have been sampled from.

Our setup differs from recent methods in ImageNav where panoramic 360° FoV sensors are required [15, 39, 46]. Here, we consider a standard 90° FoV for the agent’s view [72]. While having a complete FoV sensor simplifies localization, this strong requirement is often not available in common robotic platforms [1–3] and leads to high computational cost. This reduces the scalability and adoption of such methods by diverse agent configurations. In addition, our task setup allows our model to transfer to a diverse set of semantic navigation tasks in a plug and play fashion without the need for modifications to the target tasks (for which the literature does not use panoramic images).

View Reward It is common to use the reduced distance to the goal to reward the agent for getting closer to p_G in addition to the success reward of finding and stopping within a small distance d_s of p_G . However, while this reward proves to be quite successful for navigation tasks like point-goal, we argue it is less suited for semantic goals like images. Since the reward does not carry a signal about the semantic goal itself, the agent may fail or require much more experience in order to capture the implicit relation between the goal and the distance to goal reward (DTG). For example, if the goal shows an image of an oven, the agent may get close and stop nearby while looking at a book on the counter, and nonetheless receive a full success reward. This may lead to capturing trivial or incoherent associations between the

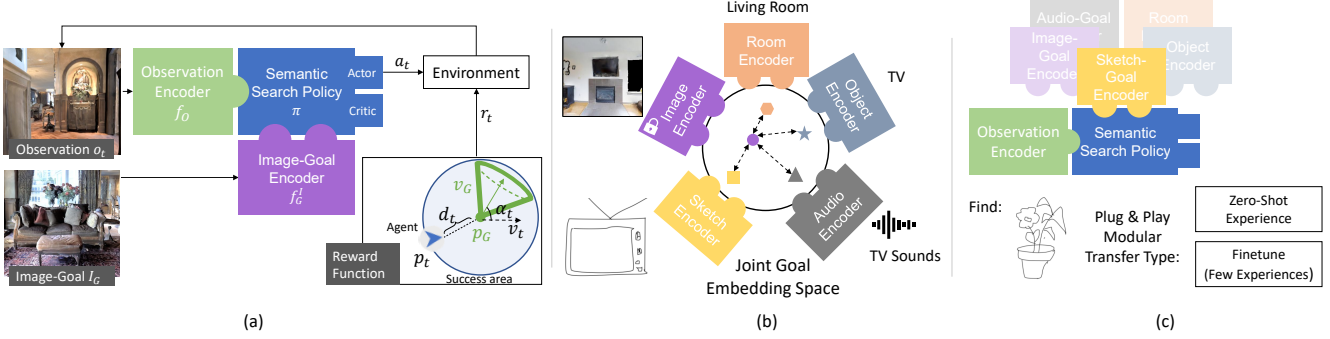


Figure 2. Our approach (a) starts by learning a semantic search policy using a novel reward function for finding random image views in a 3D scene. Then, (b) we learn a joint goal embedding space for various goal modalities where the learning is guided by the image-goal encoder. Finally, (c) we transfer our model in a plug & play fashion to a new target task where it can perform out of the box (zero-shot) or it is finetuned using few experiences on the target task.

goal and the agent’s observations.

In order to encourage the agent to leverage the information provided in the goal description I_G and effectively capture useful semantic priors that may help it in finding p_G , we propose a new reward function that rewards the agent for looking at I_G when getting closer to p_G , so it can better draw the association between its o_t and I_G . Specifically, we define the reward function at step t as:

$$r_t = r_d(d_t, d_{t-1}) + [d_t \leq d_s] r_\alpha(\alpha_t, \alpha_{t-1}) - \gamma, \quad (1)$$

where r_d is the reduced distance to the goal from the current position relative to the previous one, $[\cdot]$ is the indicator function, r_α is the reduced angle in radians to the goal view from the current view relative to the previous one, and $\gamma = 0.01$ is a slack reward to encourage efficiency. Note, this reward will encourage the agent to look at I_G when it gets near the goal, since it is rewarded to reduce the angle between its current view v_t and the view of the goal v_G (see Fig. 2a). Finally, the agent receives a maximum success reward of 10 if it reaches the goal and stops within a distance of d_s from p_G and an angle α_s from v_G :

$$R_s = 5 \times ([d_t \leq d_s] + [d_t \leq d_s \text{ and } \alpha_t \leq \alpha_s]). \quad (2)$$

We set $d_s = 1$ m (the success distance of the task) and $\alpha_s = 25^\circ$ to allow for a good overlap between v_t and v_G and enable the agent to draw the association between its observation o_t and the goal I_G .

View Augmentation In addition to the view reward introduced above, we also provide a simple task augmentation method to promote generalization by increasing the diversity of goals presented to the agent. For each training episode, rather than having a fixed I_G , we sample a view from a random angle at location p_G and provide the agent with the associated I_G from the sampled view as the goal descriptor. This has a regularization effect on the model learning; the agent will be less likely to overfit due to the changing goal description each time the agent experiences

a given goal. Furthermore, with the start p_0 and the goal location p_G fixed in the training episode but not I_G , this encourages the agent to capture implicit spatial semantic priors of things that usually appear near each other as viewed from p_G . For example, the agent would learn that an image of chairs as seen when peering from the door is likely to be at the same location of the current image goal that is showing a dining table, since the agent experienced the same episode before but with I_G showing the chairs, hence prompting the agent to explore the dining room.

Policy Training We train our policy using reinforcement learning (RL), Fig. 2a. For each training episode, we sample an image-goal I_G from p_G . The agent encodes its current observation o_t (an RGB image) with f_O and the image-goal with f_G^I and passes these encodings to the policy π . The policy further encodes these information along with the history of observations so far to produce a state embedding s_t . An actor-critic network leverages s_t to predict state value c_t and the agent’s next action a_t . Based on the agent’s state in the environment, it receives a reward (Eq. 1 and Eq. 2). The model is trained end-to-end using PPO [59].

3.2. Joint Goal Embedding Learning

Having learned the semantic search policy, we can now transfer our model to downstream tasks. Specifically, we consider downstream navigation tasks where the goals are *object categories* (ObjectNav [10]), *room types* (RoomNav [65]), or *view encodings* (ViewNav), and they may be expressed by the modalities of a label name, a sketch, an audio clip, or an edgemap; see Sec. 4.2. A key advantage of learning the semantic search policy using RGB image-goals is that these goals contain rich information about the target visual appearance and context. Furthermore, in order to solve the image-goal navigation task, our model learns to encode these visual cues via a compact dense representation produced by the image-goal encoder f_G^I .

Our idea is to leverage f_G^I to learn a joint embedding space of different goal modalities for the various tasks. In

other words, we upgrade the image-goal embedding space to be a joint goal embedding space to draw associations between the images and the different goal modalities like sketches, category names, and audio (Fig. 2b). This step can be carried out quite efficiently and using an offline dataset. For example, to learn about object-goals that are represented with a label (e.g., a chair) we only need to annotate a set of images with chairs. Then we train an object-goal encoder to produce an embedding similar to the image-goal encoder for compatible image-label pairs. In our experiments, we use offline datasets of size 20K images or less in which the “annotations” are actually automatic object detections. This is several orders of magnitude smaller than the amount of interactions usually needed to train a target-specific policy (tens to hundreds of millions) [45, 69].

Formally, let $D = \{(x_i, g_i)\}$ be a set of images x_i and their associated goals g_i , where g_i can be of any goal modality (e.g., audio, sketch, image, category name, edgemap) depending on the downstream task specifications. We learn a joint goal embedding space by minimizing the loss:

$$\mathcal{L}(x_i, g_i) = \begin{cases} 1 - \cos(f_G^I(x_i), f_G^M(g_i)), & \text{if } y_i = +1 \\ \max(0, \cos(f_G^I(x_i), f_G^M(g_i))), & \text{if } y_i = -1 \end{cases} \quad (3)$$

where $f_G^M(\cdot)$ is the new goal encoder of modality M , $\cos(\cdot, \cdot)$ is the cosine similarity between two embeddings, and y_i indicates whether the pair (x_i, g_i) is similar or not, as derived from the offline annotations (e.g., chair and a picture of a chair are similar; the audio of water dripping and a picture of the same are similar).

During goal embedding learning, we freeze f_G^I and learn f_G^M using Eq. 3 such that f_G^M learns to encode its goal similar to the corresponding image embedding from f_G^I .

3.3. Transfer and Zero-Shot Experience Learning

Having learned the semantic search policy and the joint goal embedding as described above, now we can transfer our model to downstream navigation tasks (Fig. 2c). For that, we only need to replace f_G^I with the suitable goal encoder for the task, such that:

$$a_t \sim \pi(f_O^I(o_t), f_G^M(g)). \quad (4)$$

Our plug and play modular transfer approach has multiple advantages. Since all modules are compatible with each other, this means the model can perform the target task out of the box, i.e., it does not require any further task-specific interactions to solve the target task. We refer to this setup as zero-shot experience learning (ZSEL). Training policies with modern RL frameworks is the most expensive part of the model learning, and with ZSEL we manage to circumvent this requirement. Furthermore, due to the modular nature of our approach, it is easy to generalize to a wide variety of tasks and goal modalities. For a new task, only

the respective goal encoder is trained with an offline dataset then integrated in the full model in a plug&play fashion.

Finally, our model can be easily finetuned for the downstream task to capture any additional cues specific to the task to reach a better performance. Unlike the common approach in the literature where only f_O is pretrained and transferred [23, 31, 58, 71], here the full model is transferred to the target task. This leads to higher initial performance, faster convergence, and better overall performance, as we will show in Sec. 4.

4. Evaluation

In the following experiments, we first evaluate our semantic search policy performance in the source task (image-goal navigation) compared to state-of-the-art methods (Sec. 4.1); then we show how our model transfers to a diverse set of downstream navigation tasks (Sec. 4.2).

Shared Implementation Setup For fair comparisons, we adopt the same architecture and training pipeline for our model and all RL baselines, and we note any deviations from this shared setup in the respective sections. We use a ResNet9 [33] for f_O and a GRU [21] of 2 layers and embedding size of 128 for π . For goal encoders f_G , we use a ResNet9 to encode image-, sketch-, edgemap- and audio-goal modalities. We transform an audio clip to a spectrogram before encoding it by the CNN. If the goal is a category name, we use a 2 layer MLP for f_G . We train the policy using DD-PPO [63] and allocate the same computation resources for all models. We use input augmentation (random cropping and color-jitter) during training to improve the stability and performance of the RL methods [38, 42, 46]. We adopt end-to-end RNN-based RL since it is a common [23, 31, 46, 58, 63, 71, 72], generic architecture, does not require hand-crafted modules, shows good performance on real-data [12, 47], and learned in sim has the potential to generalize well to real [35]. However, our contributions are orthogonal to the RL architecture used.

Agent Configuration The action space of the agent consists of move_forward by 25 cm, turn_left and right by 30°, and stop. The agent uses only RGB observations of 128 × 128 resolution and 90° FoV sensor.

4.1. Image-Goal Navigation

Task Setup We adopt the image-goal task as defined in Sec. 3.1. We set $S = 1000$ and $d_s = 1$ m from p_G .

Datasets We use the Habitat simulator [57] and the Gibson [66] environments to train our model. We use the dataset from [46]. The training split contains 9K episodes sampled from each of the 72 training scenes. Following the setup from [46], all RL models are trained for 50K updates (500 million frames) on the training split. The test split has 4.2K episodes sampled uniformly from 14 disjoint

Model	Split	Succ.	SPL
Imitation Learning	A	9.9	9.5
Zhu <i>et al.</i> [72]	A	19.6	14.5
Mezghani <i>et al.</i> [46]	A	9.0	6.0
DTG-RL	A	22.6	18.0
Ours	A	29.2	21.6
Ours (View Aug. Only)	A	22.0	18.8
Ours (View Reward Only)	A	24.4	17.3
Hahn <i>et al.</i> [32]	B	24.0	12.4
Ours	B	33.0	23.6
Hahn <i>et al.</i> [32] w/ noisy actuation	B	20.3	8.8
Ours w/ noisy actuation	B	25.9	17.6

Table 1. Image-goal navigation results on Gibson [66].

(unseen) scenes. For direct comparison with [32], we also test our model on a second split (“split B”) provided by [32] that has 3K episodes and the same structure as the test split from [46] (“split A”).

Baselines We compare our image-goal model to the following baselines and SoTA methods: 1) **Imitation Learning**: This model’s policy is trained using supervised learning to predict the ground truth best action on the shortest path to the goal given its current observation. 2) **Zhu *et al.* [72]**: The model uses a ResNet50 shared between f_O and f_G , pretrained on ImageNet and frozen. 3) **Mezghani *et al.* [46]**: This is the SoTA panoramic image-goal navigation model. It uses a ResNet18 for f_O and f_G , a 2 layer LSTM [34] for π , and a specialized episodic memory. We adapt this model to our 90° FoV for o_t and I_G and train it using the author’s code. 4) **DTG-RL**: This model uses the shared architecture along with the common distance to goal dense reward for training. 5) **Hahn *et al.* [32]**: This model learns from a passive dataset of videos collected from the Gibson training scenes and uses a customized architecture based on topological maps (see [32] for details).

Results and Analysis Table 4 reports the overall performance in terms of average success rate (Succ) and Success weighted by inverse Path Length (SPL) over 3 random seeds. Our model outperforms strong baselines and the SoTA in image-goal navigation by a significant margin. In split A, our model gains +6.6% in Succ and +2.6% in SPL over the best baseline. The method designed for panoramic sensors [46] tends to underperform in this challenging setting as it relies heavily on the 360° FoV for accurate localization. Furthermore, in split B, our model gains +9% in Succ and +11.2% in SPL over [32]. It is important to note that the model from [32] uses a much more complete sensor configuration than our method (pose sensor, RGB and Depth sensors of 480×640 resolution, and a 120° FoV) and it is trained offline from passive videos sampled from the simulator. Nonetheless, our model outperforms [32] by a large margin, showing that interactive learning of end-to-end RL models still has an advantage over heuristic and pas-

Model	MP3D [13]		HM3D [52]	
	Succ.	SPL	Succ.	SPL
Imitation Learning	5.3	5.1	2.0	1.9
Zhu <i>et al.</i> [72]	9.8	7.9	4.4	2.7
Mezghani <i>et al.</i> [46]	6.9	3.9	3.5	1.9
DTG-RL	11.0	9.0	5.5	3.7
Hahn <i>et al.</i> [32]	9.3	5.2	6.6	4.3
Ours	14.6	10.8	9.6	6.3

Table 2. Image-goal navigation results on MP3D and HM3D in a cross-domain evaluation setup.

sive approaches.

Ablations To validate our contributions from Sec. 3.1, we test our model performance when removing the view reward or the view augmentation. As shown in Table 4, we see a degradation in performance whenever one of these components are removed, and the largest gain is realized when they work in tandem. Additionally, we test our model under noisy actuation. While methods in split A do not provide results under noisy conditions, [32] does. Following the setup from [32], we use the noise model from [15] that simulates actions learned from a Locobot [3]. Our model shows robustness to noise and maintains its advantage over the baselines (Table 4 bottom).

Cross-Domain Generalization Next we test the models trained on Gibson on datasets from Matterport3D (MP3D) [13] and HM3D [52]. In addition to the visual domain gap between these datasets, MP3D has more complex and larger scenes than Gibson, and HM3D has high diversity in terms of scene types. This poses a very challenging cross-domain evaluation setting. The test split from each dataset has in total 3K episodes sampled uniformly from 100 and 18 scenes for HM3D and MP3D, respectively. Table 2 shows the results. Overall, we see a drop in performance for all models in this challenging setting, especially for HM3D since there is high diversity in the 100 test scenes. Nonetheless, our model outperforms all baselines on both datasets, showing that our contributions lead to better generalization by encouraging the agent to pay closer attention to the semantic information provided by the goal.

4.2. Transfer to Downstream Tasks

Tasks We consider 3 target tasks and 4 goal modalities:

1) **ObjectNav**: The agent is asked to find the nearest instance of one of 6 categories (*bed, chair, couch, potted-plant, toilet, and tv*) specified by the goal. We extend the standard ObjectNav specification [10] where the goal is given by its label (*e.g.*, find a *chair*) to goals specified by a hand drawn sketches of the category, or audio produced by the object (*e.g.*, sounds from TV). In the beginning of an episode, the agent gets either a label, a sketch, or a 4 second audio clip from a random category. An episode is successful if the agent stops within 1 m of the goal while using less

Model	Source Task	ObjectNav			RoomNav	ViewNav
		Label	Sketch	Audio	Label	Edgemap
Task Expert	-	8.0	6.7	6.6	8.9	0.8
MoCo v2 [20] (Gib.)	SSL	10.5	9.9	8.8	9.3	1.0
MoCo v2 [20] (IMN)	SSL	7.8	12.7	11.5	9.7	1.3
Visual Priors [58]	SL	9.3	9.9	9.1	13.1	0.6
Zhou <i>et al.</i> [71]	SL	15.6	7.6	9.6	10.3	0.7
CRL [23]	RL	1.9	0.5	1.0	1.2	0.0
SplitNet [31]	RL	9.0	6.5	8.8	7.7	0.6
DD-PPO (PN) [63]	RL	13.9	13.6	12.9	13.9	1.7
Ours (ZSEL)	RL	11.3	11.4	4.4	11.2	5.4
Ours	RL	21.9	22.0	18.0	27.9	7.4

Table 3. Transfer learning success rate on downstream semantic navigation tasks.

than $S = 500$ steps. For sketches, we use images of the object categories from the Sketch dataset [24]. For audio clips we sample sounds from the audio dataset in [16] and the audio heard by the agent is scaled by the distance to the goal (*i.e.*, further away goals have fainter sounds). While for label goals, the category name is the same during training and testing, for audio and sketches, the goal instances used during training are disjoint from those used in testing. This poses another challenging dimension for the agent to generalize across in addition to the unseen test scenes.

2) **RoomNav**: The agent is tasked with finding the nearest room of 6 types: *living-room*, *kitchen*, *bedroom*, *office*, *bathroom*, and *dining-room*. The goal is a label (find an *office*) and the episode is successful if the agent steps inside the room with the maximum episode length $S = 500$ [50].

3) **ViewNav**: This task is similar to the image-goal navigation task considered above, except a different modality (an edgemap) represents the goal. This helps quantify the model performance in target tasks that are more aligned with the source task but with a substantially different goal modality. In each episode, the agent receives an edgemap from a random view in the scene and needs to find the goal and stops within 1 m to succeed. We set $S = 1000$ to give the agent enough time to succeed in this challenging task.

Datasets For all target tasks, we use 24 train / 5 test scenes from the Gibson [66] tiny set that has semantic annotations [8]. These scenes are disjoint from those used in Sec. 4.1. We train all methods for up to 20 million steps on the target tasks and report evaluation performance averaged over 3 random seeds. See Supp for details.

To train the goal embedding for the modalities in ObjectNav and RoomNav, we sample 14K images of objects and 20K of rooms from the training scenes. We use the object labels generated by a model from [8] to draw the associations between the images and each modality. For ViewNav, we sample 170K views from the training scenes and generate their edgemaps using an edge texture model [70]. The number of samples for the offline dataset is driven by the

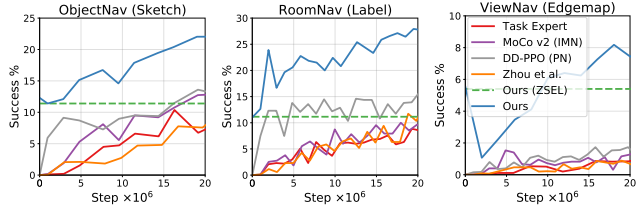


Figure 3. Transfer learning and ZSEL performance on downstream navigation tasks. See Supp for all tasks and modalities.

available instances of each goal type in the training scenes. While there is a finite number of rooms and objects, we can sample views freely from any location in a scene.

Baselines We compare our model to a set of baselines and SoTA models in transfer learning: 1) **Task Expert** which learns from scratch on the downstream task. 2) **MoCo v2 [20]** initializes f_O using MoCo training on ImageNet (IMN) or on a set of images randomly sampled from the Gibson (Gib.) training scenes. 3) **CRL [23]** pretrains f_O (ResNet50) using a combination of curiosity-based exploration and self-supervised learning. We initialize f_O from a pretrained model provided by the authors. 4) **Visual Priors [58]** uses a set of 4 ResNet50s pretrained encoders as f_O . The encoders are trained in a supervised manner to predict 4 features (*e.g.* semantic segmentation, surface normal) that provide maximum coverage for downstream navigation tasks [58]. 5) **Zhou *et al.* [71]** transfers 2 pretrained ResNet50s for depth prediction and semantic segmentation; however, unlike [58], these are used with an RGB encoder (ResNet9) trained from scratch. 6) **SplitNet [31]** pretrains f_O (customized CNN) using a mix of 6 auxiliary tasks (motion and visual tasks) and point-goal navigation. We initialize f_O from a pretrained model provided by the authors. 7) **DD-PPO (PN) [63]** pretrains the model for point-goal navigation (PN) and both f_O and π are transferred.

Transfer Learning Table 5 shows the results. Our approach outperforms all baselines by a significant margin. Interestingly, the self-supervised methods [20] reach a competitive performance to those that rely on the availability of dense annotations (like semantic segmentation and ground truth depth) for supervised representation learning [58, 71]. Furthermore, methods that learn a curiosity-based representation (CRL [23]) or via auxiliary tasks and RL (SplitNet [31]) do not transfer as well as the SSL and SL methods. Additionally, compared to the strong DD-PPO [63] approach which was trained on the same data as our policy but for the PointNav task, our model achieves substantial gains in success rate (from +5% and up to +14%) across all tasks. This indicates that our semantic search policy is much better suited to transfer to diverse downstream tasks compared to the PointNav policy. Moreover, when looking at the test performance over the course of training for the best transfer methods compared to ours (Fig. 8), we notice that our ap-

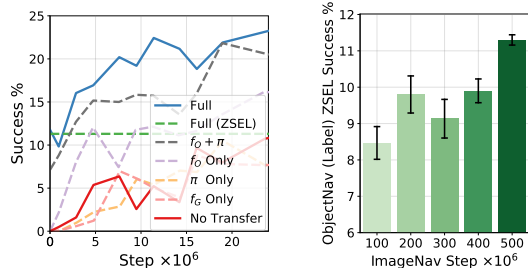


Figure 4. Our model ablation for modular transfer (left) and scalability (right).

proach has a much higher start and improves faster to better performance. Our model reaches the top performance of the best competitor up to $12.5\times$ faster.

Zero-Shot Experience Learning A unique feature of our approach is its ability to perform the downstream task without receiving any new experiences from it. Our model shows excellent performance under the challenging ZSEL setting. Our ZSEL model outperforms the Task Expert in 4 out of 5 of the tasks despite receiving zero new experience on the target, and even after training the Task Expert for up to 20 million steps (Ours-ZSEL in Table 5).

In addition, we see in Fig. 8 that the majority of transfer learning models struggle to reach our ZSEL performance. Note that our model does not have any advantages in terms of architecture, which is shared with the rest of the models. Thus the high ZSEL performance is attributable to our modular transfer approach. In ObjectNav and RoomNav, the best competitor requires between 2 to 16 million steps to reach our ZSEL performance, and with the exception of ObjectNav-Audio the competitors show little improvement over that level. In ViewNav, we notice that none of the baselines are capable of reaching our ZSEL level. This can be attributed to the challenging goal modality where estimating distances for successful stopping is difficult, and to the close proximity of this task to the source ImageNav task that our semantic policy is most familiar with.

Modular Transfer Ablation Fig. 4 (left) shows a modular ablation of our approach on the ObjectNav-Label task. Transferring individual modules separately has mixed impact on performance. While transferring f_G and π only does not improve over the ‘No Transfer’ case, f_O leads to positive transfer effect. This is expected since in this model f_O is a deep CNN with the largest portion of parameters. Having a good initialization of this components is beneficial. Nonetheless, when combining the modules together with our plug and play modular approach we see substantial gains. Our full model demonstrates the best performance and enables ZSEL, thus validating our contributions.

Scalability We evaluate our model’s ability to scale in terms of experience gathered on the source task. We find a strong correlation between the experience gathered on the source task and the ZSEL performance on downstream

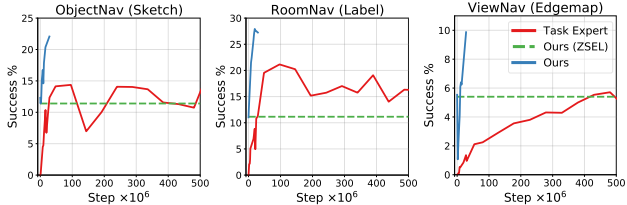


Figure 5. Long-term Task Expert training. See Supp for all tasks.

ones. As our semantic search policy receives more experience on the source task (ImageNav), its ZSEL performance on the target task gets better (Fig. 4 right). This is important since our source task requires no annotations and can be easily scaled to more scenes and large datasets. For an analysis of our model in terms of the used sensors, see Supp.

Long-Term Task Expert Training We saw above that our model scales well and its transfer improves when more experience is gathered on the source task. However, does a task expert become competitive if it simply gets longer training on the target task? How long does that model take to catch up with our approach? To find out, we train the Task Expert on each of the target tasks for up to 500M steps. Fig. 9 shows the results. The Task Expert requires on average more than 22M steps on ObjectNav and RoomNav, and up to 416M on ViewNav (in total 507M steps over the 5 tasks) to reach our ZSEL performance. It never reaches our model’s top performance when our model is finetuned on the target task. Moreover, our model reaches the best performance of the Task Expert $34.7\times$ faster. The Task Expert needs task-specific experience with task-specific annotations, which can be expensive and limits the available training data. In contrast, our model learns in the source task using more diverse goals that can be sampled randomly from the (unannotated) scene, allowing it to scale more effectively.

5. Conclusion

We introduce a plug&play modular transfer learning approach that provides a unified model for a diverse set of semantic visual navigation tasks with different goal modalities. Our semantic search policy outperforms the SoTA in the source task of image-goal navigation, as well as the SoTA in transfer learning for visual navigation by a significant margin. Furthermore, our model is able to perform new tasks effectively with zero-shot experience—to our knowledge, a completely new functionality for visual navigation. This is a stepping stone for future work, especially for tasks with high-cost training data. Being able to do ZSEL and learn from few experiences is a crucial skill for an agent in open-world and lifelong learning settings.

Acknowledgements: UT Austin is supported in part by DARPA L2M, the UT Austin IFML NSF AI Institute, and the FRL Cog Sci Consortium. Thanks to Lina Mezghani for providing access to data and code.

References

- [1] Hello Robot. <https://hello-robot.com/>. [Online]. 3
- [2] TurtleBot. <https://www.turtlebot.com/>. [Online]. 3
- [3] Locobot: An open source low cost robot. <http://www.locobot.org>, 2019. [Online]. 3, 6
- [4] Ziad Al-Halah and Rainer Stiefelhagen. Automatic Discovery, Association Estimation and Learning of Semantic Attributes for a Thousand Categories. In *CVPR*, 2017. 3
- [5] Ziad Al-Halah, Makarand Tapaswi, and Rainer Stiefelhagen. Recovering the Missing Link: Predicting Class-Attribute Associations for Unsupervised Zero-Shot Learning. In *CVPR*, 2016. 2, 3
- [6] Peter Anderson, Angel Chang, Devendra Singh Chaplot, Alexey Dosovitskiy, Saurabh Gupta, Vladlen Koltun, Jana Kosecka, Jitendra Malik, Roozbeh Mottaghi, Manolis Savva, et al. On evaluation of embodied navigation agents. *arXiv preprint arXiv:1807.06757*, 2018. 1, 2, 3
- [7] Peter Anderson, Qi Wu, Damien Teney, Jake Bruce, Mark Johnson, Niko Sünderhauf, Ian Reid, Stephen Gould, and Anton Van Den Hengel. Vision-and-language navigation: Interpreting visually-grounded navigation instructions in real environments. In *CVPR*, 2018. 15
- [8] Iro Armeni, Zhi-Yang He, JunYoung Gwak, Amir R Zamir, Martin Fischer, Jitendra Malik, and Silvio Savarese. 3D Scene Graph: A Structure for Unified Semantics, 3D Space, and Camera. In *ICCV*, 2019. 7, 12
- [9] Tim Bailey and Hugh Durrant-Whyte. Simultaneous localization and mapping (SLAM): Part II. *IEEE Robotics & Automation Magazine*, 13(3):108–117, 2006. 2
- [10] Dhruv Batra, Aaron Gokaslan, Aniruddha Kembhavi, Oleksandr Maksymets, Roozbeh Mottaghi, Manolis Savva, Alexander Toshev, and Erik Wijmans. Objectnav revisited: On evaluation of embodied agents navigating to objects. *arXiv preprint arXiv:2006.13171*, 2020. 1, 2, 4, 6
- [11] Mathilde Caron, Ishan Misra, Julien Mairal, Priya Goyal, Piotr Bojanowski, and Armand Joulin. Unsupervised learning of visual features by contrasting cluster assignments. In *NeurIPS*, 2020. 2
- [12] M. Chancán and M. Milford. MVP: Unified Motion and Visual Self-Supervised Learning for Large-Scale Robotic Navigation. *arXiv preprint arXiv:2003.00667*, 2020. 5
- [13] Angel Chang, Angela Dai, Thomas Funkhouser, Maciej Halber, Matthias Niessner, Manolis Savva, Shuran Song, Andy Zeng, and Yinda Zhang. Matterport3D: Learning from RGB-D Data in Indoor Environments. *International Conference on 3D Vision (3DV)*, 2017. Matterport3D license available at http://kaldir.vc.in.tum.de/matterport/MP_TOS.pdf. 2, 6, 12
- [14] Devendra Singh Chaplot, Lisa Lee, Ruslan Salakhutdinov, Devi Parikh, and Dhruv Batra. Embodied multimodal multi-task learning. *IJCAI*, 2020. 2
- [15] Devendra Singh Chaplot, Ruslan Salakhutdinov, Abhinav Gupta, and Saurabh Gupta. Neural topological slam for visual navigation. In *CVPR*, 2020. 1, 2, 3, 6
- [16] Changan Chen, Ziad Al-Halah, and Kristen Grauman. Semantic Audio-Visual Navigation. In *CVPR*, 2021. 2, 7, 12
- [17] Changan Chen, Unnat Jain, Carl Schissler, Sebastia Viçenc Amengual Gari, Ziad Al-Halah, Vamsi Ithapu, Philip W Robinson, and Kristen Grauman. SoundSpaces: Audio-Visual Navigation in 3D Environments. In *ECCV*, 2020. 1, 2
- [18] Changan Chen, Sagnik Majumder, Ziad Al-Halah, Ruohan Gao, Santhosh K. Ramakrishnan, and Kristen Grauman. Learning to Set Waypoints for Audio-Visual Navigation. In *ICLR*, 2021. 2
- [19] Ting Chen, Simon Kornblith, Mohammad Norouzi, and Geoffrey Hinton. A simple framework for contrastive learning of visual representations. In *ICML*, 2020. 2
- [20] Xinlei Chen, Haoqi Fan, Ross Girshick, and Kaiming He. Improved baselines with momentum contrastive learning. *arXiv preprint arXiv:2003.04297*, 2020. 2, 7, 15
- [21] Kyunghyun Cho, Bart Van Merriënboer, Dzmitry Bahdanau, and Yoshua Bengio. On the properties of neural machine translation: Encoder-decoder approaches. In *Eighth Workshop on Syntax, Semantics and Structure in Statistical Translation (SSST-8)*, 2014. 5
- [22] Jia Deng, Wei Dong, Richard Socher, Li-Jia Li, Kai Li, and Li Fei-Fei. Imagenet: A large-scale hierarchical image database. In *CVPR*, 2009. 2
- [23] Yilun Du, Chuang Gan, and Phillip Isola. Curious Representation Learning for Embodied Intelligence. In *ICCV*, 2021. 2, 5, 7, 15
- [24] Mathias Eitz, James Hays, and Marc Alexa. How Do Humans Sketch Objects? *ACM Trans. Graph. (Proc. SIGGRAPH)*, 31(4):44:1–44:10, 2012. 7, 12
- [25] Mohamed Elhoseiny, Babak Saleh, and Ahmed Elgammal. Write a classifier: Zero-shot learning using purely textual descriptions. In *ICCV*, 2013. 3
- [26] Benjamin Eysenbach, Abhishek Gupta, Julian Ibarz, and Sergey Levine. Diversity is All You Need: Learning Skills without a Reward Function. In *ICLR*, 2018. 2
- [27] Chelsea Finn, Pieter Abbeel, and Sergey Levine. Model-agnostic meta-learning for fast adaptation of deep networks. In *ICML*, 2017. 2
- [28] Jorge Fuentes-Pacheco, José Ruiz-Ascencio, and Juan Manuel Rendón-Mancha. Visual simultaneous localization and mapping: a survey. *Artificial Intelligence Review*, 43(1):55–81, 2015. 2
- [29] Chuang Gan, Yiwei Zhang, Jiajun Wu, Boqing Gong, and Joshua B Tenenbaum. Look, Listen, and Act: Towards Audio-Visual Embodied Navigation. In *ICRA*, 2020. 1
- [30] Ross Girshick, Jeff Donahue, Trevor Darrell, and Jitendra Malik. Rich feature hierarchies for accurate object detection and semantic segmentation. In *CVPR*, 2014. 2
- [31] Daniel Gordon, Abhishek Kadian, Devi Parikh, Judy Hoffman, and Dhruv Batra. SplitNet: Sim2Sim and Task2Task Transfer for Embodied Visual Navigation. In *ICCV*, 2019. 2, 5, 7, 15
- [32] Meera Hahn, Devendra Chaplot, Mustafa Mukadam, James Rehg, Shubham Tulsiani, and Abhinav Gupta. No RL, No Simulation: Learning to Navigate without Navigating. In *NeurIPS*, 2021. 6, 12, 13

- [33] Kaiming He, Xiangyu Zhang, Shaoqing Ren, and Jian Sun. Deep Residual Learning for Image Recognition. In *CVPR*, 2016. 5
- [34] Sepp Hochreiter and Jürgen Schmidhuber. Long Short-Term Memory. *Neural Computation*, 9(8):1735–1780, 1997. 6
- [35] Abhishek Kadian, Joanne Truong, Aaron Gokaslan, Alexander Clegg, Erik Wijmans, Stefan Lee, Manolis Savva, Sonia Chernova, and Dhruv Batra. Sim2real predictivity: Does evaluation in simulation predict real-world performance? *IEEE Robotics and Automation Letters*, 5(4):6670–6677, 2020. 5
- [36] Diederik P Kingma and Jimmy Ba. Adam: A method for stochastic optimization. In *ICLR*, 2015. 12
- [37] Eric Kolve, Roozbeh Mottaghi, Winson Han, Eli VanderBilt, Luca Weihs, Alvaro Herrasti, Daniel Gordon, Yuke Zhu, Abhinav Gupta, and Ali Farhadi. AI2-THOR: An Interactive 3D Environment for Visual AI. *arXiv*, abs/1712.05474, 2017. 2
- [38] Ilya Kostrikov, Denis Yarats, and Rob Fergus. Image augmentation is all you need: Regularizing deep reinforcement learning from pixels. In *ICLR*, 2021. 5
- [39] Obin Kwon, Nuri Kim, Yunho Choi, Hwiyeon Yoo, Jeongho Park, and Songhwai Oh. Visual Graph Memory with Unsupervised Representation for Visual Navigation. In *ICCV*, 2021. 3
- [40] Christoph H Lampert, Hannes Nickisch, and Stefan Harmeling. Learning to detect unseen object classes by between-class attribute transfer. In *CVPR*, 2009. 2, 3
- [41] Hugo Larochelle, Dumitru Erhan, and Yoshua Bengio. Zero-data Learning of New Task. In *AAAI*, 2008. 3
- [42] Michael Laskin, Kimin Lee, Adam Stooke, Lerrel Pinto, Pieter Abbeel, and Aravind Srinivas. Reinforcement learning with augmented data. In *NeurIPS*, 2020. 5
- [43] Juncheng Li, Xin Wang, Siliang Tang, Haizhou Shi, Fei Wu, Yueting Zhuang, and William Yang Wang. Unsupervised reinforcement learning of transferable meta-skills for embodied navigation. In *CVPR*, 2020. 2
- [44] Tsung-Yi Lin, Michael Maire, Serge Belongie, James Hays, Pietro Perona, Deva Ramanan, Piotr Dollár, and C Lawrence Zitnick. Microsoft coco: Common objects in context. In *ECCV*, 2014. 2
- [45] Oleksandr Maksymets, Vincent Cartillier, Aaron Gokaslan, Erik Wijmans, Wojciech Galuba, Stefan Lee, and Dhruv Batra. THDA: Treasure Hunt Data Augmentation for Semantic Navigation. In *ICCV*, 2021. 3, 5
- [46] Lina Mezghani, Sainbayar Sukhbaatar, Thibaut Lavril, Oleksandr Maksymets, Dhruv Batra, Piotr Bojanowski, and Kartheek Alahari. Memory-Augmented Reinforcement Learning for Image-Goal Navigation. *arXiv*, 2021. 3, 5, 6, 13
- [47] Piotr Mirowski, Matt Grimes, Mateusz Malinowski, Karl Moritz Hermann, Keith Anderson, Denis Teplyashin, Karen Simonyan, Koray Kavukcuoglu, Andrew Zisserman, and Raia Hadsell. Learning to navigate in cities without a map. In *NeurIPS*, 2018. 5
- [48] Arsalan Mousavian, Alexander Toshev, Marek Fišer, Jana Košecká, Ayzaan Wahid, and James Davidson. Visual representations for semantic target driven navigation. In *ICRA*, 2019. 2
- [49] Matthias Müller, Alexey Dosovitskiy, Bernard Ghanem, and Vladlen Koltun. Driving policy transfer via modularity and abstraction. In *CoRL*, 2018. 2
- [50] Medhini Narasimhan, Erik Wijmans, Xinlei Chen, Trevor Darrell, Dhruv Batra, Devi Parikh, and Amanpreet Singh. Seeing the un-scene: Learning amodal semantic maps for room navigation. In *ECCV*, 2020. 1, 7
- [51] Santhosh K. Ramakrishnan, Ziad Al-Halah, and Kristen Grauman. Occupancy Anticipation for Efficient Exploration and Navigation. In *ECCV*, 2020. 2
- [52] Santhosh K Ramakrishnan, Aaron Gokaslan, Erik Wijmans, Oleksandr Maksymets, Alex Clegg, John Turner, Eric Undersander, Wojciech Galuba, Andrew Westbury, Angel X Chang, et al. Habitat-Matterport 3D Dataset (HM3D): 1000 Large-scale 3D Environments for Embodied AI. In *NeurIPS Datasets and Benchmarks Track (Round 2)*, 2021. HM3D license available at <https://matterport.com/matterport-end-user-license-agreement-academic-use-model-data>. 2, 6, 12
- [53] Santhosh K Ramakrishnan, Tushar Nagarajan, Ziad Al-Halah, and Kristen Grauman. Environment Predictive Coding for Embodied Agents. In *ICLR*, 2022. 2
- [54] Marcus Rohrbach, Michael Stark, and Bernt Schiele. Evaluating knowledge transfer and zero-shot learning in a large-scale setting. In *CVPR*, 2011. 3
- [55] Nikolay Savinov, Alexey Dosovitskiy, and Vladlen Koltun. Semi-parametric topological memory for navigation. In *ICLR*, 2018. 1
- [56] Manolis Savva, Angel X. Chang, Alexey Dosovitskiy, Thomas Funkhouser, and Vladlen Koltun. MINOS: Multimodal indoor simulator for navigation in complex environments. *arXiv:1712.03931*, 2017. 1
- [57] Manolis Savva, Abhishek Kadian, Oleksandr Maksymets, Yili Zhao, Erik Wijmans, Bhavana Jain, Julian Straub, Jia Liu, Vladlen Koltun, Jitendra Malik, Devi Parikh, and Dhruv Batra. Habitat: A Platform for Embodied AI Research. In *ICCV*, 2019. 1, 2, 5, 12
- [58] Alexander Sax, Jeffrey O Zhang, Bradley Emi, Amir Zamir, Silvio Savarese, Leonidas Guibas, and Jitendra Malik. Learning to navigate using mid-level visual priors. In *CoRL*, 2019. 2, 5, 7, 15
- [59] John Schulman, Filip Wolski, Prafulla Dhariwal, Alec Radford, and Oleg Klimov. Proximal policy optimization algorithms. *arXiv preprint arXiv:1707.06347*, 2017. 4
- [60] Ramanan Sekar, Oleh Rybkin, Kostas Daniilidis, Pieter Abbeel, Danijar Hafner, and Deepak Pathak. Planning to Explore via Self-Supervised World Models. In *ICML*, 2020. 3
- [61] Sebastian Thrun. Probabilistic robotics. *Communications of the ACM*, 45(3):52–57, 2002. 2
- [62] Xin Eric Wang, Vihan Jain, Eugene Ie, William Yang Wang, Zornitsa Kozareva, and Sujith Ravi. Environment-agnostic multitask learning for natural language grounded navigation. In *ECCV*, 2020. 2
- [63] Erik Wijmans, Abhishek Kadian, Ari Morcos, Stefan Lee, Irfan Essa, Devi Parikh, Manolis Savva, and Dhruv Batra. DD-PPO: Learning Near-Perfect PointGoal Navigators from 2.5 Billion Frames. In *ICLR*, 2020. 2, 3, 5, 7, 12, 15

- [64] Mitchell Wortsman, Kiana Ehsani, Mohammad Rastegari, Ali Farhadi, and Roozbeh Mottaghi. Learning to learn how to learn: Self-adaptive visual navigation using meta-learning. In *CVPR*, 2019. [2](#)
- [65] Yi Wu, Yuxin Wu, Aviv Tamar, Stuart Russell, Georgia Gkioxari, and Yuandong Tian. Bayesian Relational Memory for Semantic Visual Navigation. In *ICCV*, 2019. [1](#), [2](#), [4](#)
- [66] Fei Xia, Amir R. Zamir, Zhi-Yang He, Alexander Sax, Jitendra Malik, and Silvio Savarese. Gibson Env: Real-World Perception for Embodied Agents. In *CVPR*, 2018. Gibson license available at http://svl.stanford.edu/gibson2/assets/GDS_agreement.pdf. [2](#), [5](#), [6](#), [7](#), [12](#), [13](#)
- [67] Yongqin Xian, Bernt Schiele, and Zeynep Akata. Zero-shot learning-the good, the bad and the ugly. In *CVPR*, 2017. [2](#), [3](#)
- [68] Wei Yang, Xiaolong Wang, Ali Farhadi, Abhinav Gupta, and Roozbeh Mottaghi. Visual semantic navigation using scene priors. In *ICLR*, 2019. [2](#)
- [69] Joel Ye, Dhruv Batra, Abhishek Das, and Erik Wijmans. Auxiliary Tasks and Exploration Enable ObjectGoal Navigation. In *ICCV*, 2021. [5](#)
- [70] Amir R Zamir, Alexander Sax, William Shen, Leonidas J Guibas, Jitendra Malik, and Silvio Savarese. Taskonomy: Disentangling task transfer learning. In *CVPR*, 2018. [2](#), [7](#)
- [71] Brady Zhou, Philipp Krähenbühl, and Vladlen Koltun. Does computer vision matter for action? *Science Robotics*, 2019. [2](#), [5](#), [7](#), [15](#)
- [72] Yuke Zhu, Roozbeh Mottaghi, Eric Kolve, Joseph J Lim, Abhinav Gupta, Li Fei-Fei, and Ali Farhadi. Target-driven Visual Navigation in Indoor Scenes using Deep Reinforcement Learning. In *ICRA*, 2017. [1](#), [2](#), [3](#), [5](#), [6](#), [13](#)

6. Supplementary Materials

Additional information presented in this supplementary:

1. Details on the shared implementation (Sec. 7).
2. Details of the image-goal navigation dataset (Sec. 8).
3. Detailed results on image-goal navigation across 3 levels of episode difficulties (Table 4).
4. Examples of the visual goal modalities used in target tasks (Fig. 6).
5. Dataset details for the target tasks and goal embedding space (Sec. 9).
6. Detailed results with standard deviations on target tasks (Table 5).
7. Qualitative results for our model in all tasks and goal modalities (Fig. 10).
8. Examples of failure cases for our model (Fig. 11).
9. Performance curves for all tasks and goal modalities in transfer learning setup (Fig. 8) and long-term training of Task Expert (Fig. 9).
10. Ablation on the sensor configuration used by the agent (Fig. 7)
11. Discussion of potential societal impact (Sec. 10) and limitations (Sec. 11).

7. Shared Setup

All RL methods are trained with the following setup. We use input augmentation of random cropping and color jitter for both observations and goals. The models are trained with DD-PPO [63]. We set the number of PPO epochs 2, the forward steps 128, the entropy coefficient 0.01, clipping of 0.2, and train the model end-to-end using the Adam optimizer [36]. We allocate the same number of processes and resources to all methods.

We use the Habitat simulator [57] along with the Gibson [66], Matterport3D [13], and HM3D [52] datasets. These datasets are photorealistic and scans of real-world environments with varying complexities, sizes, room layouts, types. In all our experiments, the test scenes are disjoint from those used for training to assess the agent ability to generalize to previously unseen environments.

8. Image-Goal Navigation

Dataset The training split contains 9K episodes sampled from each of the 72 Gibson training scenes. The episodes are uniformly split across 3 levels of difficulty based on the goal’s geodesic distance from the start location: *easy*(1.5 - 3 m), *medium*(3 - 5 m), and *hard*(5 - 10 m). Test split A has 4.2K episodes and split B has 3K episodes. Both splits are sampled uniformly from 14 disjoint (unseen) scenes and the 3 levels of difficulty. Further, to avoid trivial straight line

paths, the episodes has a minimum geodesic to euclidean distance ratio of 1.1 in A and 1.2 in B (our split B corresponds to the curved split in [32]).

Detailed Results We show in Table 4 the detailed results of all models across the three levels of episode difficulties (*easy*, *medium* and *hard*). Our model shows better performance across the different levels and in both split A and B. For a qualitative result, see Fig. 10 A.

9. Transfer Learning to Downstream Tasks

Datasets We use 29 scenes from Gibson and split them into 24 scenes for training and 5 for testing. In the following, we present the details of the datasets used for each of the downstream tasks.

- ObjectNav: We sample 24K episodes for training and 1K episodes for testing. For the sketch-goals (Fig. 6 middle), we sample 80 sketches from [24] for each object category and split them to 70 used during training and 10 for testing. For the audio-goals, we sample 12 audio clips from [16] of lengths ranging from 13 to 53 seconds and split them 50/50 for training and testing. At the start of each episode of the ObjectNav (Audio) task a random 4 seconds duration is sampled from the respective audio clip and split, and presented to the agent as the goal descriptor.
- RoomNav: We sample 25K episodes for training and 290 for testing.
- ViewNav: We sample 24K episodes for training and 1.5K for testing. We generate edgmaps for 300 random views per scene and we randomly assign one of those per episode as the goal (Fig. 6 right).

Goal Embedding Space In the joint goal embedding space, we aim to learn goal encoders that are compatible to the image-goal encoder. For example, an image view from a living room with a tv detected in it will be used as the positive anchor for a sketch of a tv, a sound clip from a tv, the tv label, the living room label, and the edgmap of the view. The annotations for the sampled image view are based on model predictions from [8]. During training, the parameters of f_G^I are kept frozen and we train the various goal encoders defined in Sec.4 using the loss from Main/Sec.3.2.

Detailed Results for All Tasks In Table 5 we show the average success rate and standard deviation for all methods over 3 random seeds. Fig. 8 shows the performance of the best transfer learning methods and our approach across all tasks and goal modalities. Fig. 9 shows the Task Expert performance when trained for up to 500M steps on each of the respective tasks and in comparison to our model performance under the ZSEL setting or when it is finetuned. Furthermore, we show example navigation episodes from

Model	Split	Easy		Medium		Hard		Overall	
		Succ.	SPL	Succ.	SPL	Succ.	SPL	Succ.	SPL
Imitation Learning	A	18.5	17.7	8.4	8.1	2.6	2.6	9.9	9.5
Zhu <i>et al.</i> [72]	A	31.7	25.1	15.7	10.8	11.5	7.5	19.6	14.5
Mezghani <i>et al.</i> [46]	A	17.5	11.0	8.8	6.6	0.6	0.5	9.0	6.0
DTG-RL	A	32.9	26.2	21.2	17.0	13.6	10.8	22.6	18.0
Ours	A	39.7	28.5	29.6	22.5	18.2	13.8	29.2	21.6
Ours (View Aug. Only)	A	37.0	31.7	18.5	15.9	10.7	9.0	22.0	18.8
Ours (View Reward Only)	A	32.3	22.7	24.8	18.1	16.1	11.0	24.4	17.3
Hahn <i>et al.</i> [32]	B	35.5	18.4	23.9	12.1	12.5	6.8	24.0	12.4
Ours	B	48.0	34.2	36.0	25.9	15.1	10.8	33.0	23.6
Hahn <i>et al.</i> [32] w/ noisy actuation	B	27.3	10.6	23.1	10.4	10.5	5.6	20.3	8.8
Ours w/ noisy actuation	B	41.0	28.2	27.3	18.6	9.3	6.0	25.9	17.6

Table 4. Detailed results across 3 levels of difficulties on image-goal navigation in Gibson [66].

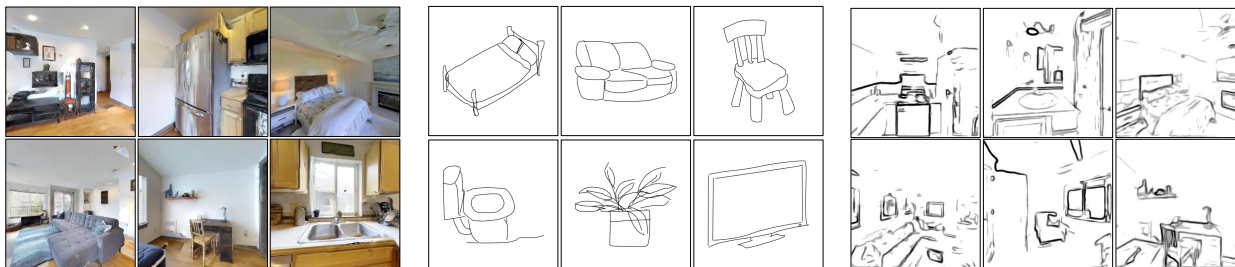


Figure 6. Examples of visual goals used for the target navigation tasks: left) ImageNav (Image), middle) ObjectNav (Sketch), right) ViewNav (Edgemap).

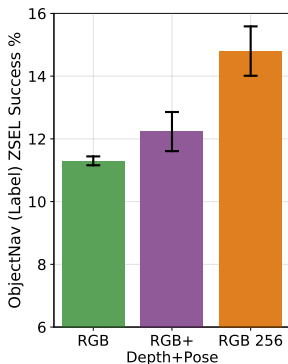


Figure 7. Scalability ablation for our model when changing the sensors configuration.

all tasks and goal modalities for our approach in Fig. 10. Our plug and play modular transfer learning approach enable our model to perform diverse set of tasks effectively.

Scalability (Sensors) We evaluate our model’s ability to scale across the sensor suite. Fig. 7 shows our model performance when varying the sensors configuration in the source task (ImageNav) and evaluating on ObjectNav (Label) under the ZSEL setup. As expected, when enriching the agent sensors to include depth and pose sensors in addition to

vision, we see an additional improvement in performance. More importantly, when increasing the vision sensor resolution from 128 to 256 we see a significant bump in ZSEL success rate that exceeds the one from diversifying the sensory suite. Our model seems to benefit from an enhanced vision channel as it carries the important semantic cues needed for our semantic search policy and goal embedding space.

Failure Cases We show in Fig. 11 few examples of failure cases encountered by our model. We notice that some of these failure cases are related to the type of the goal modality. For example, in ImageNav the agent sometimes finds the object described in the image however misestimate the view point the image is taken from, hence stops a bit far from the goal location (Fig. 11 A). In ViewNav (Edgemap), the goal modality lacks distinctive texture and color information which leads the agent to sometime stops at a location with similar edge structure but it is actually not the goal (Fig. 11 B). A type of failure cases spotted in multiple tasks are the early stopping cases. In these cases, the agent fails to estimate the distance to the goal correctly and stops early resulting in an unsuccessful episode (Fig. 11 C).

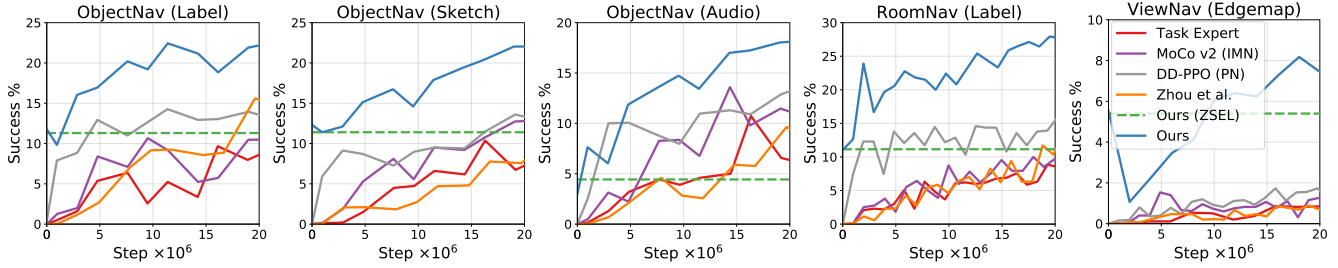


Figure 8. Transfer learning and ZSEL performance on downstream navigation tasks.

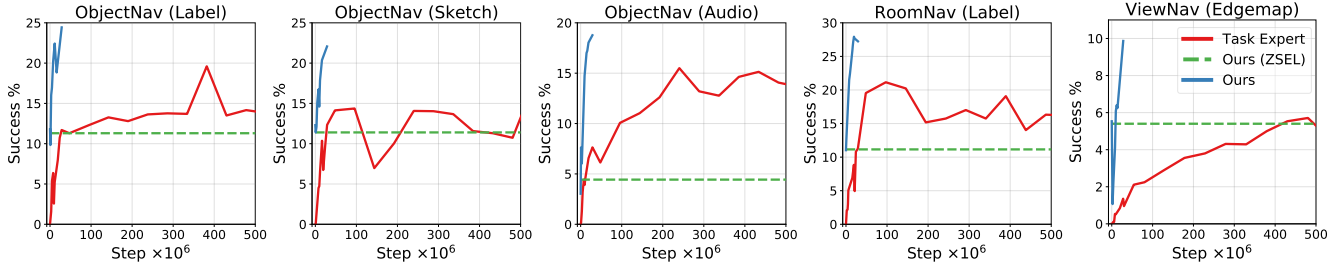


Figure 9. Long-term Task Expert training. Our model maintains its superior performance even when the Task Expert is presented with extensive experience in the target task.

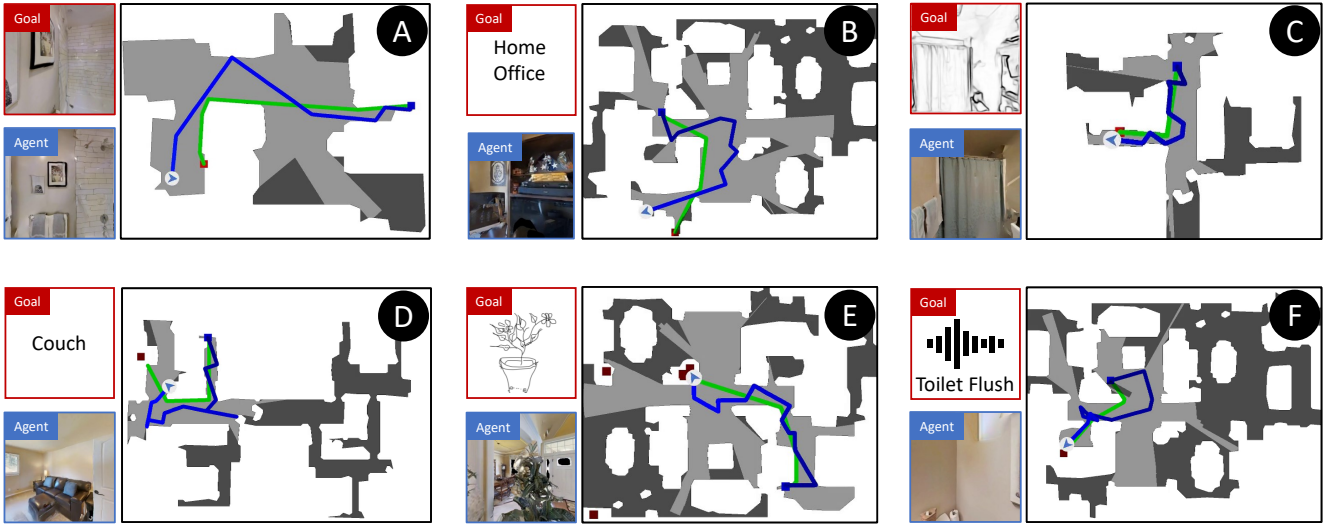


Figure 10. Qualitative results of our approach performing 6 tasks with 5 goal modalities: A) ImageNav (Image), B) RoomNav (Label), C) ViewNav (Edgemap), D) ObjectNav (Label), E) ObjectNav (Sketch), F) ObjectNav (Audio).



Figure 11. Qualitative results of failure cases in A) ImageNav (Image), B) ViewNav (Edgemap), and C) ObjectNav (Label).

Model	Source Task	Label	ObjectNav		RoomNav	ViewNav
			Sketch	Audio	Label	Edgemap
Task Expert	-	8.0 \pm 0.6	6.7 \pm 1.4	6.6 \pm 0.7	8.9 \pm 0.8	0.8 \pm 0.3
MoCo v2 [20] (Gib.)	SSL	10.5 \pm 0.7	9.9 \pm 0.6	8.8 \pm 1.2	9.3 \pm 0.9	1.0 \pm 0.2
MoCo v2 [20] (IMN)	SSL	7.8 \pm 0.3	12.7 \pm 0.8	11.5 \pm 0.8	9.7 \pm 2.2	1.3 \pm 0.3
Visual Priors [58]	SL	9.3 \pm 0.1	9.9 \pm 0.7	9.1 \pm 0.8	13.1 \pm 0.9	0.6 \pm 0.1
Zhou <i>et al.</i> [71]	SL	15.6 \pm 1.0	7.6 \pm 0.3	9.6 \pm 0.8	10.3 \pm 0.9	0.7 \pm 0.1
CRL [23]	RL	1.9 \pm 0.5	0.5 \pm 0.3	1.0 \pm 0.4	1.2 \pm 0.8	0.0 \pm 0.0
SplitNet [31]	RL	9.0 \pm 1.0	6.5 \pm 0.8	8.8 \pm 1.1	7.7 \pm 1.1	0.6 \pm 0.0
DD-PPO (PN) [63]	RL	13.9 \pm 0.6	13.6 \pm 0.8	12.9 \pm 0.5	13.9 \pm 1.6	1.7 \pm 0.1
Ours (ZSEL)	RL	11.3 \pm 0.2	11.4 \pm 0.6	4.4 \pm 0.6	11.2 \pm 1.3	5.4 \pm 0.6
Ours	RL	21.9 \pm 0.1	22.0 \pm 0.9	18.0 \pm 1.2	27.9 \pm 1.9	7.4 \pm 0.1

Table 5. Transfer learning average success rate and standard deviation on downstream semantic navigation tasks.

10. Potential Societal Impact

Our approach’s application domain is semantic visual navigation. Here, autonomous agents are trained to find semantic objects in a 3D environment. Such a technology can have positive societal impact by improving people’s life, especially in domains like elder care, with robots that can aid in daily life tasks (*e.g.* find my keys, go to the bedroom and bring me my medicine). On the other side, the datasets used in this study are 3D scans of building and houses from certain geographic and cultural areas (western style houses from well-off areas). This creates certain biases in the type of building architectures, room, and object types the agent is familiar with. Consequently, this may limit the availability of this technology to a small section of the population. More diverse datasets and methods with robust adaptation to strong shifts in building layouts and object types are needed to mitigate these effects.

11. Discussion and Limitations

We propose a novel approach for modular transfer learning that enables the agent to handle multiple tasks with diverse goal modalities effectively. Our model can solve the downstream tasks out-of-the-box in zero-shot experience learning setup alleviating the need for expensive interactive training of the policy. Alternatively, our model can be finetuned on the downstream task to learn task-specific cues where it showed to learn faster, generalize better and reach higher performance than the baselines. While we focused in this work on semantic navigation tasks, this can be seen as a first step in this exciting direction. Additional research is needed to generalize this method to tasks that require a series of goals and a compatible policy that can plan effectively in a multi-goal setup (*e.g.* VLN [7]). Further, our results and evaluation demonstrate strong transfer learning performance for our method. However, as usual in transfer learning, there is not a theoretical guarantee that a transfer

effect will always be beneficial. Target tasks with significant differences to the source task may not benefit from transferring the accumulated experience in the source.